Journal of Scientific & Industrial Research
Vol. 68, March 2009, pp.203-213

Effect of impeller-diffuser radial gap ratio in a centrifugal pump

Adnan Ozturk[1], Kadir Aydin[2], Besir Sahin[2] and Ali Pinarbasi[1]*

[1]Cumhuriyet University, Engineering Faculty, Mechanical Engineering Department, Sivas, 58140, Turkey

[2]Cukurova University, Engineering Faculty, Mechanical Engineering Department, Adana, Turkey

Received 13 May 2008; revised 26 December 2008; accepted 31 December 2008

In this study, effects of flow behavior in a non-traditional centrifugal pump, whose diffuser was subjected to different radial gaps, were investigated numerically using multi-purpose FLUENT code. Flow was assumed to be three dimensional, viscous and incompressible. $k-\varepsilon$ RNG with standard near-wall functions was used. Centrifugal pump had a five backward curved-bladed impeller running at 890 rpm and a nine vaned diffuser. Investigations for three different radial gaps (10%, 15%, 20%) have been carried out for 15 different volume flow rates. For present pump, 20% radial gap is found most suitable for pressure fluctuations.

Keywords*:* CFD, Centrifugal pump, Impeller-diffuser interaction, Numerical simulation

Introduction

Effects of individual variables, including number of impeller blades, inlet diameter, and impeller exit width, on pump performance are difficult to predict from empirical rules[1]. Miner *et al*[2] found that distribution of relative velocity components within impeller and volute of a centrifugal pump varies with circumferential angle relative to volute cutwater. Liu *et al*[3] found that flow rate from each impeller passage varied with volute circumferential position by up to 25%. Several researchers[4-7] have concerned with diffuser action. Some internal flow studies, which revealed presence of a jet-wake structure at discharge of centrifugal rotors, were concerned with compressors[8-11]. However, Krain[12] found a velocity profile, which is different from jet-wake type flow. El Hajem *et al*[13] observed a jet-wake structure developed at impeller exit. Sinha *et al*[14,15] conducted PIV (particle image velocity) measurements to investigate flow structure and turbulence in a centrifugal pump with a vaned diffuser. Cao *et al*[16] numerically investigated to understand flow pattern through impeller of centrifugal pump under design and off-design operating conditions. Chen & Liaw[17] used a computational method to solve 3D Reynolds-Averaged flow field of an impeller in volute.

*Author for correspondence
E-mail: pinarbasi.ali@gmail.com

This paper presents a numerical study impeller-diffuser interaction considering 3D steady flow (Fig. 1) in various radial gap (20%, 15%, and 10% of impeller radius).

Proposed Model

Centrifugal pump surface model was generated using GAMBIT commercial software. Pump had 5 backward curved blades and 9 diffuser vanes. It was designed for PIV analysis, and had a constant volute thickness. Main characteristics of pump were: rotor/impeller (D_{i1} / D_{i2}, 8.51 / 20.32 cm; Z_i, 5 backward-curved; β_{i2}, 21.3); diffuser/stator (Z_d, 9; D_{d1} / D_{d2}, 24.45 / 30.5 cm; β_{d1}/ β_{d2}, 10.6° / 10.97°; L, 13.44 cm; D_{dSS}, 14.15 cm; D_{dPS}, 24.79 cm; T, 1.27 cm); experimental conditions (N, 890 rpm; Q^*, 5.67 l/s; ϕ^*, 0.118; N_s, 0.49); flow rate, 2.52-3.78 l/s; and flow rate coefficient range, 0.052-0.078.

Software package [FLUENT] was used for calculation with transport equations being solved using a finite volume method (FVM). Unstructured hexahedral cells were generated to define inlet (37824 cells) and outlet zones (14184 cells), while tetrahedral cells were used to define impeller (45420 cells) and volute (112118 cells). Model size (209546 cells and 153634 nodes) is not enough for a precise boundary layer simulation but it gives correct values for pump performance. In a pump, skewness factor of grid should exceed 0.80. As generated model (Fig. 2), which was assumed to have a skewness

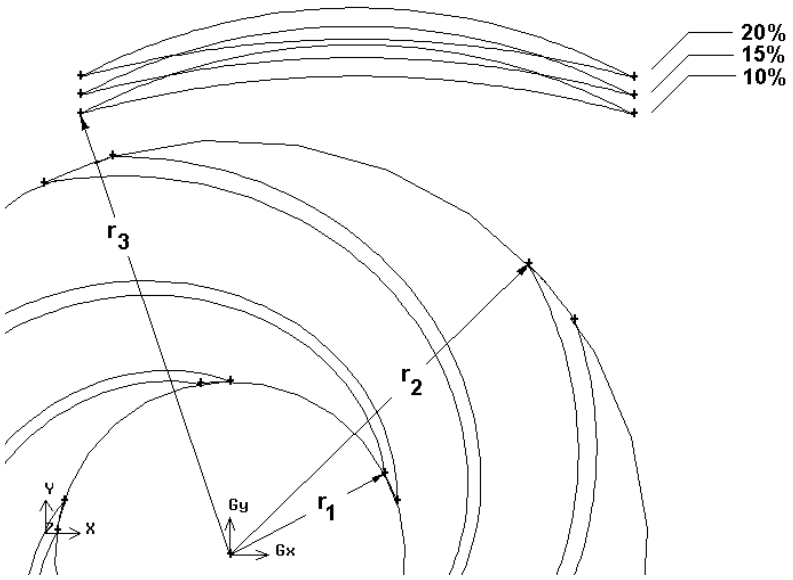


Fig. 1—Positions of impeller-diffuser and gaps

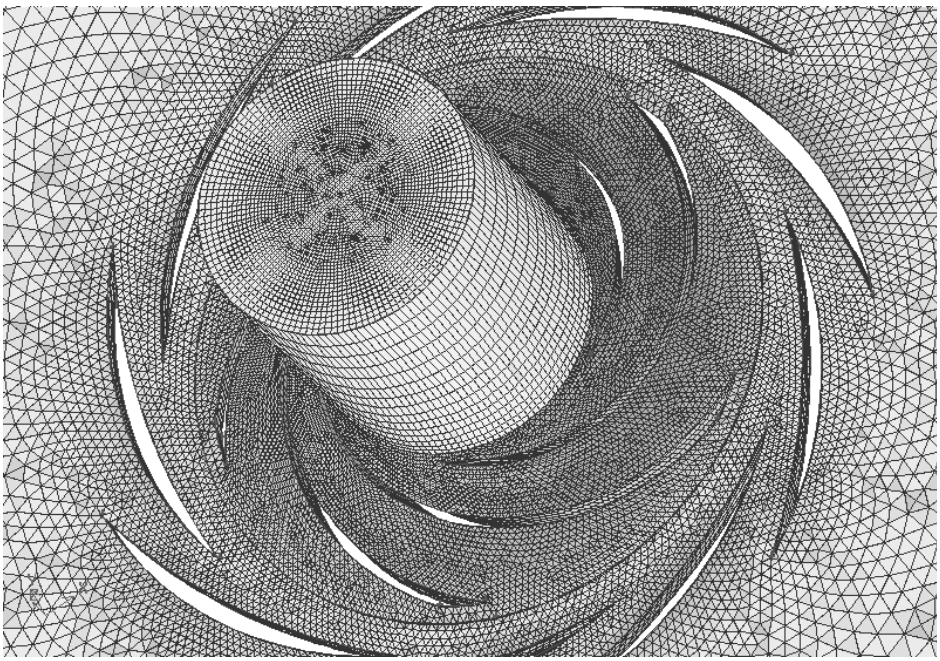


Fig. 2—Three-dimensional grid model for impeller

factor of 0.85, had no problem with grid quality. In addition to this, only skewness that exceeds 0.7 consists of only 0.24 % of cells.

Code solves Reynolds averaged Navier-Stokes equation in a primitive variable form. Turbulence effects were modeled using standard $k-\varepsilon$ turbulence model. Modeled boundary conditions selected had more physical meaning for turbomachinery flow simulations, that is, constant static pressure at the outlet and a variable flow rate proportional to kinetic energy at inlet to impeller (Fig. 3). Flow rate is changed by modifying kinetic energy at inlet condition, which simulates

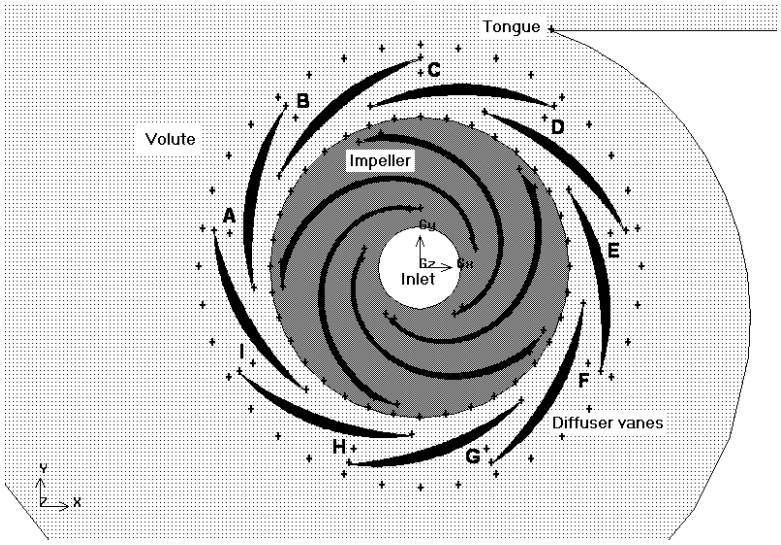


Fig. 3—Locations of static pressure just after impeller and diffuser

different closing valve positions. Also, non-slip boundary conditions have been imposed over impeller blades and diffuser vanes, volute casing and inlet pipe wall.

Numerical Solution Control

All performance curves of pump were obtained. Analysis was performed for more than 15 mass flow rate levels. When flow rate increases, analysis converges significantly, but lower flow rate level (1.93-4.55%) displays more unstable results due to stalled region effects. Higher flow rate level convergence is closer to 0.72%. Thus, in rotating stall region, flow does not converge as smoothly when compared to higher flow rates due to unstable flow phenomena effects. However, within stalled region, analysis ran for 2 or even 3 days, with a Pentium III-1000 Mhz. Outlet pressure fluctuates after approx. 100-150 iterations. After 2 or 3 days, iteration number reaches 2000-2500. As an estimation of pressure gain in stalled regime, average pressure values are assumed at iteration range from 100 to 2500.

Materials and Methods

FLUENT commercial software package uses FVM and solves 3D NSEs with ability to handle unstructured grids, include relative reference frames and steady or unsteady calculations. NSEs and associated equations are converted into algebraic form on a mesh that defines geometry and flow domain of interest and solved on discretized mesh, which defines elements in control-volumes. Time dependent term scheme is second order implicit. Pressure velocity couplings are calculated through SIMPLEC algorithm. Second order, upwind discretizations, have been used for convection terms and central difference schemes for diffusion terms.

Governing Equations

Mass Conservation Equation

Equation for conservation of mass, or continuity equation, can be written as

$$\frac{\partial \rho}{\partial t} + \nabla .(\rho \vec{v}) = S_m \qquad \ldots(1)$$

Eq. (1) is general form of mass conservation equation and is valid for incompressible as well as compressible flows. Source S_m is mass added to continuous phase from dispersed second phase due to vaporization of liquid droplets and any user-defined sources.

Momentum Conservation Equations

Conservation of momentum in an inertial (non-accelerating) reference frame is

$$\frac{\partial}{\partial t}(\rho \vec{v}) + \nabla .(\rho \vec{v} \vec{v}) = -\nabla p + \nabla .(\bar{\bar{\tau}}) + \rho \vec{g} + \vec{F} \qquad \ldots(2)$$

where, p is static pressure, $\bar{\bar{\tau}}$ is stress tensor and $\rho\vec{g}$ and $\vec{F}$ are gravitational body force and external body forces. $\vec{F}$ also contains other model-dependent source terms such as porous-media and user-defined sources. Stress tensor $\bar{\bar{\tau}}$ is given as

$$\bar{\bar{\tau}} = \mu\left[(\nabla\vec{v} + \vec{v}^{T}) - \frac{2}{3}\nabla.\vec{v}I\right] \quad \ldots(3)$$

where μ is molecular viscosity, I is unit tensor, and second term on right hand side is effect of volume dilation.

Transport Equations

Integral form of general transport equation for mass, momentum, energy, etc. can be applied to each cell as

$$\underbrace{\frac{\partial}{\partial t}\int \rho\phi dV}_{\text{Unsteady}} + \underbrace{\int \rho\phi\vec{V}\,.dA}_{\text{Convection}} = \underbrace{\int \Gamma\nabla\phi\,.dA}_{\text{Diffusion}} + \underbrace{\int S_{\phi}dV}_{\text{Generation}} \quad \ldots(4)$$

where ϕ is a variable that is used to describe a general transportable quantity and takes on different values, depending on transport equation to be solved.

Modeling of Flow

FLUENT allows to solve rotating frame problems using absolute velocity, $\vec{v}$, or relative velocity, $\vec{v}_r$, as dependent variable. Two velocities are related as

$$v_r = \vec{v} - (\vec{\Omega}\times\vec{r}) \quad \ldots(5)$$

where, $\vec{\Omega}$ is angular velocity vector (angular velocity of rotating frame) and $\vec{r}$ is position vector in rotating frame. Left hand side of momentum equations appears as follows for an inertial reference frame:

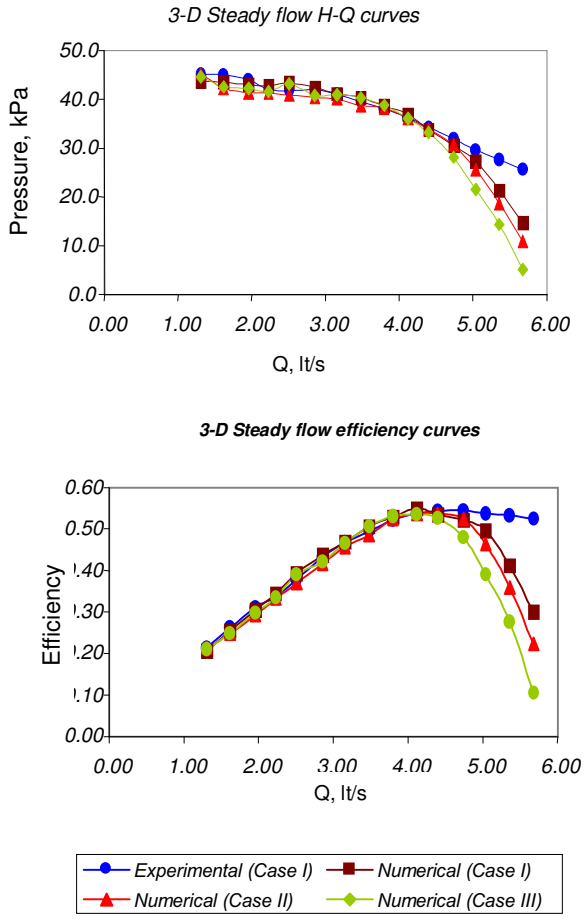


Fig. 4—Experimental and numerical curves on pump performance

$$\frac{\partial}{\partial t}(\rho\vec{v}) + \nabla.(\rho\vec{v}\vec{v}) \quad \ldots(6)$$

For a rotating reference frame, left hand side written in terms of absolute velocities becomes

$$\frac{\partial}{\partial t}(\rho\vec{v}) + \nabla.(\rho\vec{v}_r\vec{v}) + (\vec{\Omega}\times\vec{v}) \quad \ldots(7)$$

In terms of relative velocities, left-hand side is given as

$$\frac{\partial}{\partial t}(\rho\vec{v}_r) + \nabla.(\rho\vec{v}_r\vec{v}_r) + \rho(2\vec{\Omega}\times\vec{v}_r + \vec{\Omega}\times\vec{\Omega}\times\vec{r}) + \rho(\frac{\partial\vec{\Omega}}{\partial t}\times\vec{r}) \quad \ldots(8)$$

where, $2\vec{\Omega}\times\vec{v}_r + \vec{\Omega}\times\vec{\Omega}\times\vec{r}$ is Coriolis force.

Results and Discussion

Evaluation of Performance Curve

To determine performance curves, volume flow rate measurements were made varying from zero flow to maximum delivery. Computed and experimental

performance and efficiency curves (Fig. 4) were made for three different gap positions (Case I, 20%; Case II, 15%; Case III, 10%). Though numerical and experimental data were found in good agreement but disagreements increased significantly when flow rate increased. Lower volume flow rate (2.23-2.51 l/s) displays more unstable results due to stalled region effects. Thus in rotating stall region, flow does not converge as smoothly when compared with higher flow rates due to unstable flow phenomena effects. However, by further increasing flow rate, performance curves begin diverge due to unstable effects and increasing of turbulence. Best efficiency versus flow rate is described as BEP ($Q = 4.12$ l/s, $\eta = 0.5491$) in centrifugal pump (Fig. 4).

Effect of Gap Distance

Computation results deal with static pressures, velocity vectors and turbulent kinetic energy (TKE) distributions within pump (Fig. 5) at design volume flow rate (4.12 l/s) in Case I. Inlet radial velocity indicate that boundary layers developed on diffuser vanes is in agreement with reported[15] observation corresponding to flow rate at 4.12 l/s. Maximum velocity is observed at blade edges and low velocity at pump inlet.

Static pressure that increases in radial direction (Fig. 5) and pressure at suction side of impeller blades is lower, whereas it is higher at pressure side. Higher pressure contours levels, which are observed in the region between tongue and diffuser, display more irregular behavior around leading edge. Separation point on diffuser walls is expanded towards trailing edge. Static pressure in impeller passage increases gradually from inlet to exit of impeller and drops rapidly at suction side of impeller blade. Irregularity of pressure at tongue is seen from flow in rotating impeller as an unsteady boundary condition, affecting resulting fluctuations in pressure field. Similar observation could be seen at velocity vectors (Fig. 5). Jet-wake type flow phenomena exist within diffuser blades where high velocity distributions on pressure side of diffuser vanes exist while low energy fluid covered on suction side.

TKE reach maximum value at trailing edge of impeller. As pressure decreases, flow separates due to blade thickness and reduction in energy intensity. These values decrease through impeller, but increase through diffuser vanes, and continue to increase from diffuser vanes to outlet, reaching maximum at trailing edge of diffuser vanes near tongue, showing little fluctuations at pump outlet regions (Fig. 5, Case I). This is because increase in kinetic energy due to decrease in distance between tongue and diffuser vane. As impeller rotates, fluid drawing into passage of impeller blades accelerates radially outwards. On the other hand, as fluid moves through passage of diffuser blades, kinetic energy of fluid is reduced while pressure energy is further increased. As fluid flows through diffuser vanes, kinetic energy of turbulence decreases since velocities decrease. While observing velocity vectors around periphery of tongue, fluid is seen stabilized between diffuser vanes and tongue. Also, pressure is high at the same region. Jet between diffuser vanes is seen clearly. Fluid moves to pump outlet due to jet flow. Increase in loses of hitting and hurling in tongue region can be observed from TKE contours (Fig. 5).

Static pressures are considerably smaller near tongue and at exit, whereas somewhat far upstream of tongue are slightly higher when compared at three gap positions (Case I, Case II and Case III). Similar to blade impact, pressure decreases everywhere, in exit region when vane lines up with tip of tongue. Pressure maxima occur simultaneously when blade is past tip of tongue and vane is still far upstream of it (Fig. 5). Dominant effect of gap distance on static pressure and TKEs is evident within impeller, impeller diffuser interaction, and diffuser. Radial velocity at pressure side of impeller blade is higher. High radial outward velocity on pressure side is because absolute radial velocity corresponding to jet in this region is greater than passage averaged flow. Therefore, velocity distributions show a reverse flow from pressure side to suction side of blade, highlighting jet-wake phenomenon. There is sharp increase of phase averaged velocity (primarily tangential) across wake of impeller blade.

Same flow characteristics are also observed heading to exit jet flow. Maximum TKE occurs along jet flow. Thus transition between high and low velocity regions also occurs along wake line of impeller blade. Decreasing gap ratio has a significant effect on TKE. Low level of TKE was observed in Case I, and high levels of TKE obtained in Cases II and III with respect to radial gap distance. Effect of pressure drop at smaller radial gap ratio is also discernable in pressure contours by comparing for three pumps geometries. Jet-wake flow type is traced at velocity vector but effect diminished by gap distance. Flow squeezed within this part of the pump. In this region, kinetic energy level is displayed to be higher in magnitude, but, drops significantly as

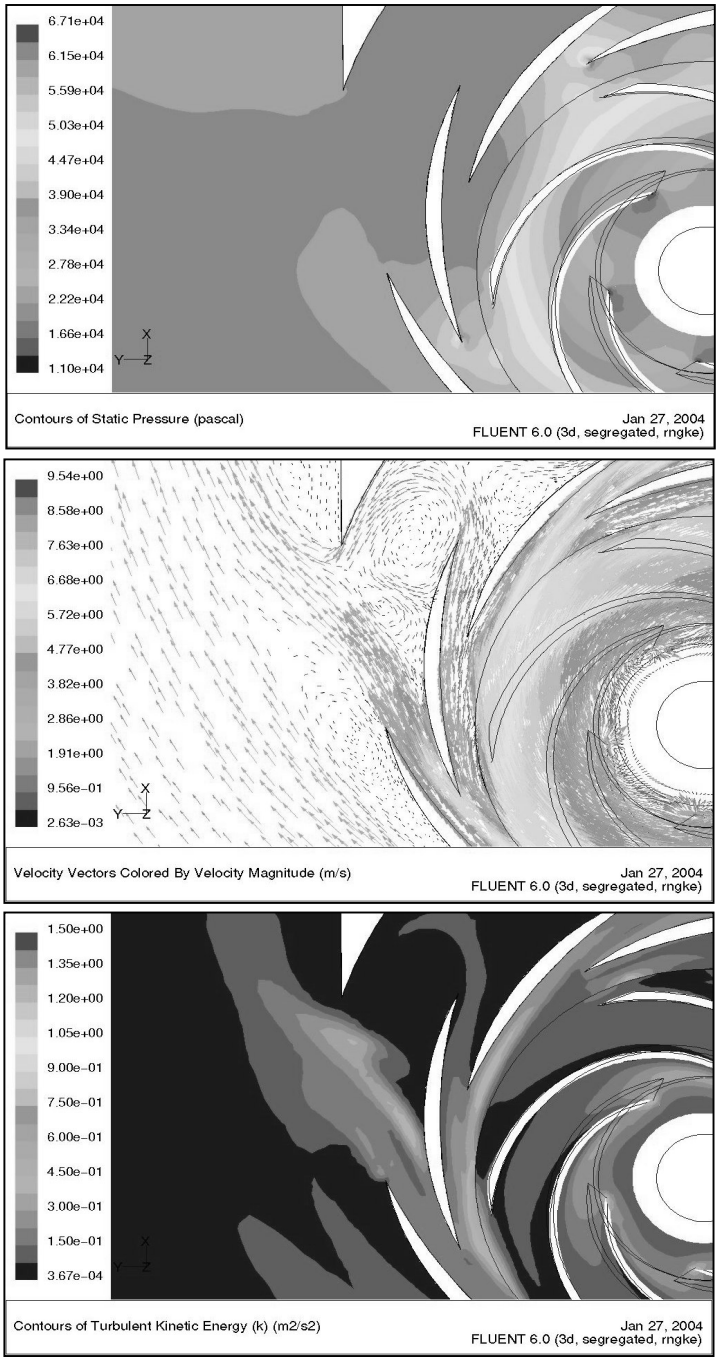


Fig. 5—Contours of static pressure, velocity vectors and turbulent kinetic energies at 20 % radial gap in Case I

gap increases. In most cases, flow field at diffuser exit is more homogeneous at smaller radial gaps indicating better diffusion, due to decrease of radial gap that is leading to unloading of highly loaded vane at diffuser exit.

Equilibrium between pressure forces and Coriolis forces in main flow is lost in boundary layers at hub and shroud surfaces, leading to a secondary flow in boundary layers directed from pressure to suction side. In main flow, a reverse secondary flow direction doesn't seem to influence static pressure distributions. Within diffuser, deterministic kinetic energy is particularly high along convex side of vane (Fig. 5) and it extends well downstream of vane along its wake. For Case III, tongue

effects are dominated by irregularities in outflux from diffuser. Thus, it is likely that any reduction in jet-wake phenomenon would have a direct impact on decreasing radial gap distance. TKE level has also observed higher than previous cases. Flow squeezing affected resulting of uniformities in impeller.

Pressure Fluctuations

Pressure fluctuations were calculated at impeller outlet, between diffuser vanes, and after diffuser (Fig. 3). Depending on radial gap between impeller blades and diffuser vanes, R_3 / R_2=1.2, 1.15 and 1.10 for 15 flow rates level. Impeller-diffuser interaction and interaction effect of different gaps are investigated by comparison of pressure fluctuations. Angular origin is at the edge of x-axis and it increases with counterclockwise orientation and tongue is at 61° (Fig. 1). The results are obtained at mid-vane height (4 mm) like experimental study to minimize effect on flow of hub, shroud and volute; this distance is half of volute thickness.

Because of non-axisymmetric geometry of volute and effect of diffuser exit of impeller, circumferential pressure variation imposes at impeller outlet. This creates a cyclic variation of flow in impeller channels and produces variable blade forces and a radial force on impeller shaft, causing failure of blades. Improvement of centrifugal pump performance and control of circumferential variation of static pressure caused by volute require a good understanding of flow mechanisms defining three-dimensional structure of flow in volute. Because radial fluid forces are generated from rotating pressure waves, whirling direction of fluid forces will be same as rotating direction of pressure waves. When rotating direction of pressure waves is same as that of impeller, fluid forces will be a forward-whirling excitation.

Magnitude of fluctuations varies significantly during one impeller revolution, due to varying distance between impeller blade trailing edge and diffuser vane leading edges as impeller completes one revolution. Trailing edge pressure fluctuations are largest during vane passage following smallest gap between specific instrumented impeller blade and diffuser vanes. Minimum pressure at trailing edge pressure top within each diffuser vane passage is attained after impeller blade trailing edge has passed diffuser vane leading edge. Pressure fluctuating at trailing edge rises sharply to its maximum value, which is attained before impeller blade trailing edge reaches next vane leading edge.

Wake causes pressure pulsations, which in turn gives rise to vibration and noise. Pressure pulsations are strongly affected by radial gap between impeller and diffuser. Largest pressure fluctuation occurs right before the pressure side of impeller blade trailing edge reaching diffuser vane leading edge. Pressure decreases sharply and reaches minimum as suction side of blade trailing edge reaches vane leading edge. Then, pressure rises sharply as impeller blade moves away from vane leading edge. Hence, most of pressure fluctuations occur during a rather short time, corresponding to about one third of impeller blade passage period. Magnitude of pressure fluctuations is defined as difference between maximum and minimum pressure value in averaging period, which corresponds to one impeller revolution. Similar calculations were made after impeller, within diffuser blades, and after diffuser. Radial gap between impeller tip and inlet edge of stator vanes is 20% of impeller radius (Case I).

Pressure fluctuations in tongue region is a minimum for the best efficiency flow rate range, and it increases rapidly for both lower and higher flow rates, in accordance with available experimental data (Fig. 6). Largest fluctuations occur at vane leading edge and on the front half of vane suction side. Those fluctuations are of the same order of magnitude as total pressure rise across the pump. Fluctuations that are larger on vane suction than on vane pressure side, decrease monotony on vane pressure side from leading edge to trailing edge.

Large pressure fluctuations on front of half of the suction side, at leading edge, and on pressure side closest to leading edge decrease significantly with increasing radial gap. Increasing radial gap between impeller blades and diffuser vanes resulted in decreasing fluctuations (Fig. 7). Magnitude of fluctuations varies significantly during one impeller revolution, due to varying distance between impeller blade trailing edge and diffuser vane leading edges as impeller completes one revolution. Trailing edge pressure fluctuations are largest during vane passage following smallest gap between impeller blade and diffuser vanes. Minimum pressure at trailing edge within each diffuser vane passage is attained after impeller blade trailing edge has passed diffuser vane leading edge. Trailing edge pressure then rises sharply to its maximum value, which is attained before impeller blade trailing edge reaches next vane leading edge. Highest pressure fluctuations occur with vaned diffuser and at suction side of stator vanes. In general, pressure fluctuations are comparatively small in design flow rate.

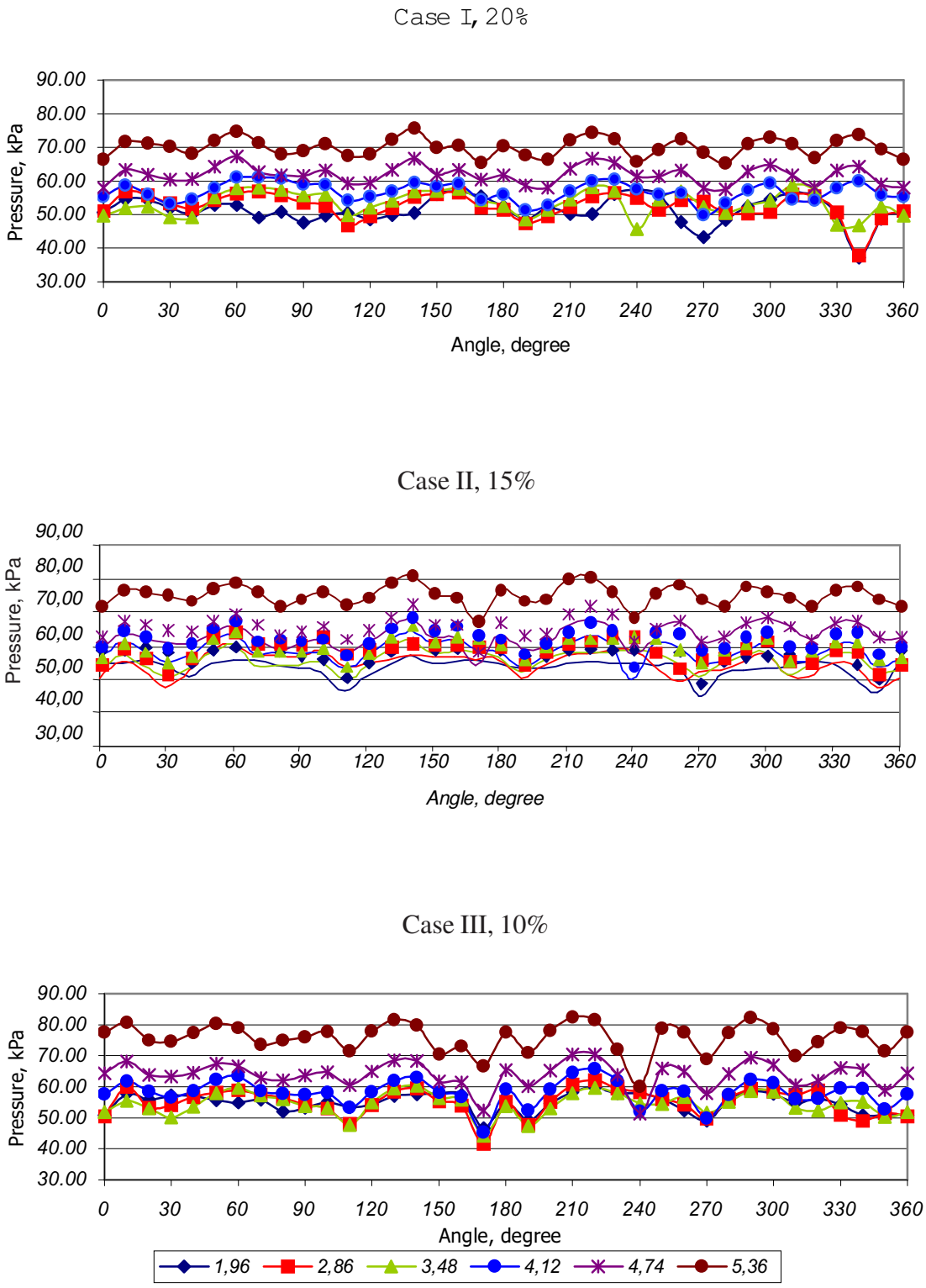


Fig. 6. Pressure fluctuations at blade passing frequency at impeller exit for Case I, II, III at 6 different volume flow rates

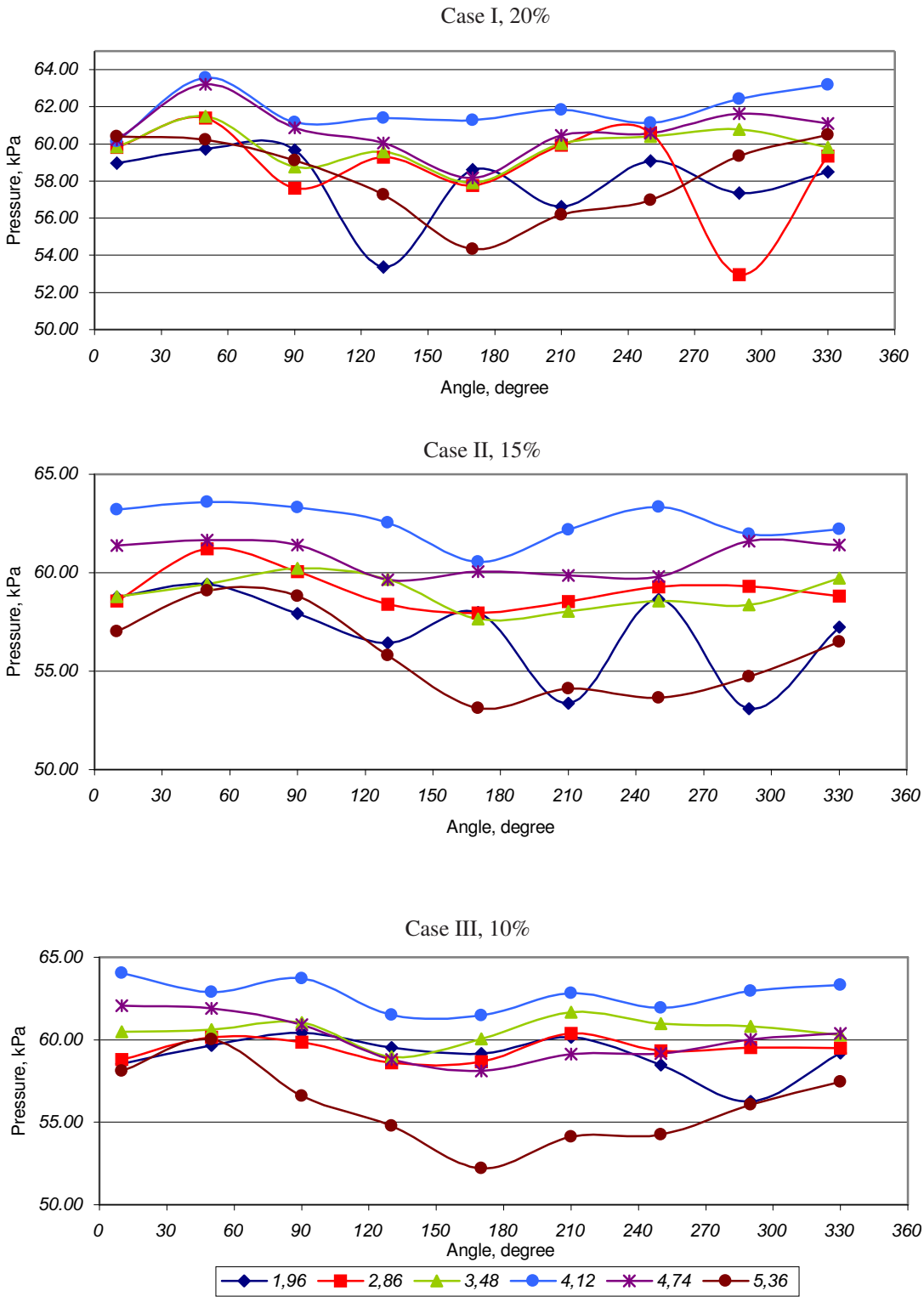


Fig. 7—Pressure fluctuations at blade passing frequency among diffuser vanes for Case I, II, III at 6 different volume flow rates

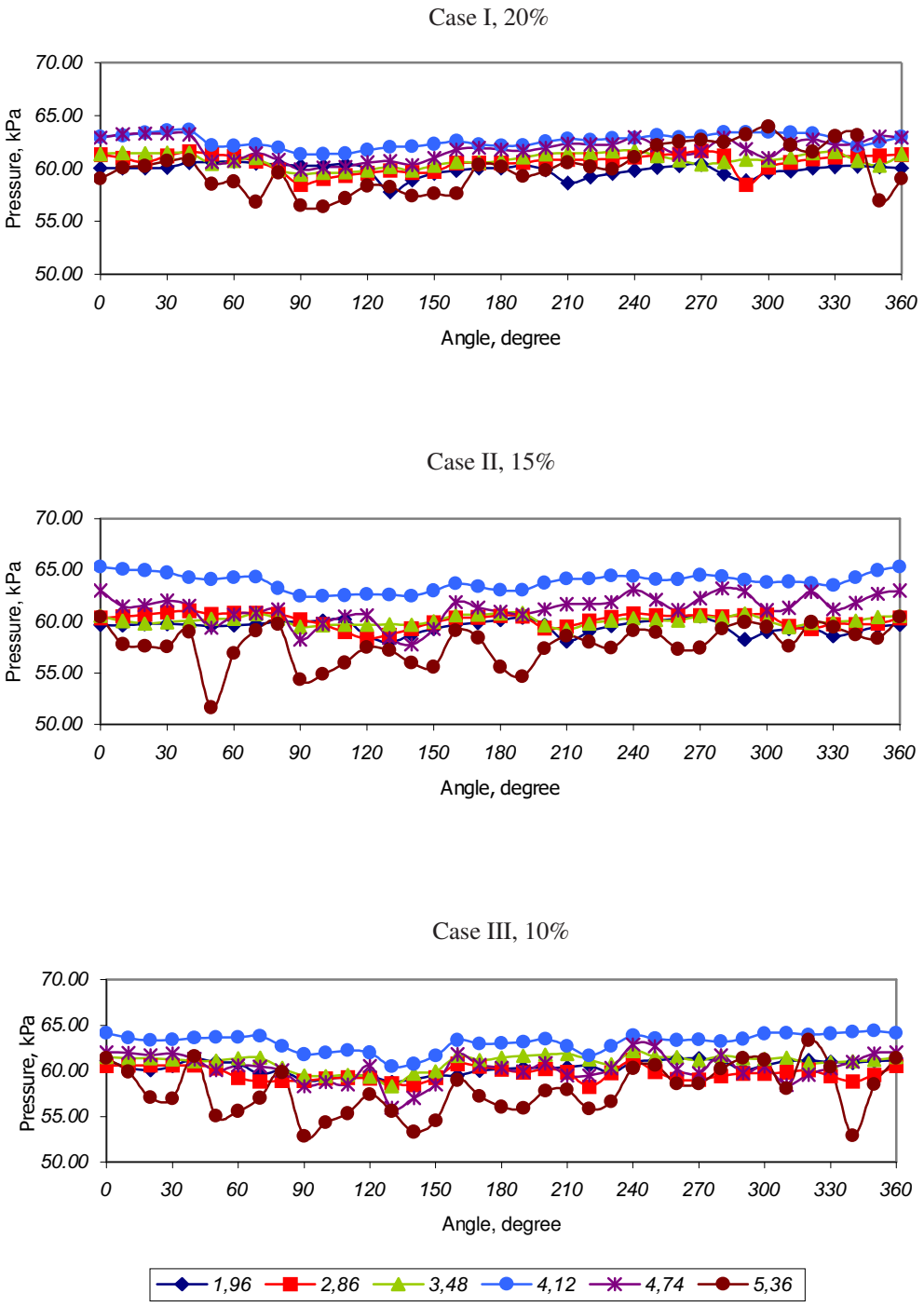


Fig. 8—Pressure fluctuations at blade passing frequency after diffuser for Case I, II, III at 6 different volume flow rates

Diffuser produces a strong effect, especially at the region after diffuser (Fig. 8). Pressure fluctuations are increased at low and high flow rates, but at nominal flow rate. For off-design conditions, however, volute region close to tongue presents a simultaneous evolution of pressure fluctuations, with big amplitude in whole region, due to strong interaction between impeller and diffuser, which produces pressure oscillations. Along volute after

diffuser, these oscillations are progressively reduced due to divergence and absorption.

Thus, pressure fluctuations in after the impeller, diffuser and between impeller and diffuser are effective based on performance and efficiency. Effects of impeller-diffuser interaction are particularly important for off-design conditions. Fluctuating pressure field extends to dynamic forces causing fatigue on pump shaft. Once pressure predictions have been proven to be quite accurate, numerical model developed has shown its worth and can be used to calculate these forces. Pressure fluctuations registered around tongue and diffuser were closely dependent on flow rate and radial gap ratios. Comparison of present data shows that reducing radial gap leads to an increase in pressure fluctuations, which change with flow rates and radial gap ratios (Figs 6-8). Near tongue and exit, pressure fluctuations are considerably smaller, whereas slightly higher at somewhat far upstream of tongue.

Conclusions

Performance curve for centrifugal pumps shows a good approximation with experimental results under FLUENT solver. Jet-wake flow pattern clearly discernable inside impeller and diffuser channels chancing magnitude of size by flow rate level. This phenomena display how complex flow dominates in pump flow by comparing velocity contours and turbulent kinetic energies especially higher value accumulated around impeller blade tips and diffuser inlet region. Jet-wake flow pattern has affected significantly by changing diffuser gap distance. When gap ratio decreases, jet is influenced within diffuser because of flow squeezing in small gap region. Flow is roughly stabilized inside tongue region. On the contrary, decreasing gap ratio, which resulted in more irregularities around diffuser walls side, expands wake form. Pump efficiency has also little affected by the impeller-diffuser gap distance which decreases in the design flow rate conditions. Largest vane pressure fluctuations occurred on vane suction side close to leading edge. For large volume flow rates, magnitude of those fluctuations reached to a maximum value in Case III. Decreasing radial gap between impeller blades and diffuser vanes, a significant increase in pressure fluctuations along front half of vane suction side resulted. Largest blade pressure fluctuations occurred at impeller blade trailing edge.

Acknowledgement

Authors thank Cukurova University Research Council (Grant FBE2002D127) for financial support and encouragement.

References

1 Tuzson J, *Centrifugal Pump Design* (Wiley and Sons, New York) 2000.

2 Miner S M & Beaudoin R D, Laser velocimetery measurements in a centrifugal pump, *ASME J Turbomach*, **111** (1989) 205-212.

3 Liu C H, Vafidis C & Whitelaw J H, Flow characteristics of a centrifugal pump, *ASME J Fluids Engg*, **116** (1994) 303-309.

4 Inoue M & Cumpsty N A, Experimental study of centrifugal impeller discharge flow in vaneless and vaned diffusers, *ASME J Engg Gas Turbines Power*, **106** (1984) 455-467.

5 Sideris M T & Van Dam Braembussche R A, Influence of a circumferential exit pressure distortion on the flow in an impeller and diffuser, *ASME J Turbomach*, **9** (1987) 48-54.

6 Arndt N, Acosta A J, Brennen C E & Caughey T K, Rotor/stator interaction in a diffuser pump, *ASME J Turbomach*, **111** (1989) 213-221.

7 Arndt N, Acosta A J, Brennen C E & Caughey T K, Experimental investigation of rotor-stator interaction in a centrifugal pump with several vaned diffusers, *ASME J Turbomach*, **112** (1990) 98-108.

8 Eckardt D, Detailed flow investigations within a high-speed centrifugal compressor impeller, *ASME J Fluids Engg*, **88** (1976) 390-402.

9 Johnston J P & Dean R C, Losses in vaneless diffusers of centrifugal compressors and pumps, *ASME J Engg Power*, **88** (1966) 49-62.

10 Rohne K H & Banzhaf M, Investigation of the flow at the exit of unshrouded centrifugal impeller and comparison with the classical jet-wake theory, *ASME J Turbomach*, **113** (1991) 654-659.

11 Ubaldi M, Zunino P, Barigozzi G & Cattanei A, An experimental investigation of stator induced unsteadiness on centrifugal impeller out-flow, *ASME J Turbomach*, **118** (1996) 41-54.

12 Krain H, Swirling impeller flow, *ASME J Turbomach*, 110 (1988) 122-128.

13 El Hajem M, Morel R, Champagne J H & Spettel F, Centrifugal impeller flow investigation, *ASME Fluids Engg Div Summer Meet*, 1998.

14 Sinha M & Katz J, Flow structure and turbulence in a centrifugal pump with a vaned diffuser, in *ASME Proc Fluids Engg Div Summer Meet*, 1998.

15 Sinha M, Pinarbasi A & Katz J, The flow structure during onset and developed states of rotating stall within a vaned diffuser of a centrifugal pump, *J Fluids Engg*, **123** (2001) 490-499.

16 Cao S, Goukas A, Wu Y, Tsukamoto H, Peng G, Liu W, Zhao L & Cao B, Three-dimensional turbulent flow in a centrifugal pump impeller under design and off-design operating conditions, *ASME Fluids Engg Div Summer Meet*, 1999.

17 Chen S H & Liaw Lu-Fu, Flow field calculations of a centrifugal pump with volute, in *Proc 1997 ASME Int Gas Turbine & Aeroengine Congr & Expo*, 1997.